

Synthesis of Bis(2,6-Diadamantyl Aryloxide) Ln(II) Complexes of Samarium, Europium, and Ytterbium and Their Ln(III) Precursors

Lauren M. Anderson-Sanchez, Joseph W. Ziller, and William J. Evans*



Cite This: *Inorg. Chem.* 2024, 63, 21416–21422



Read Online

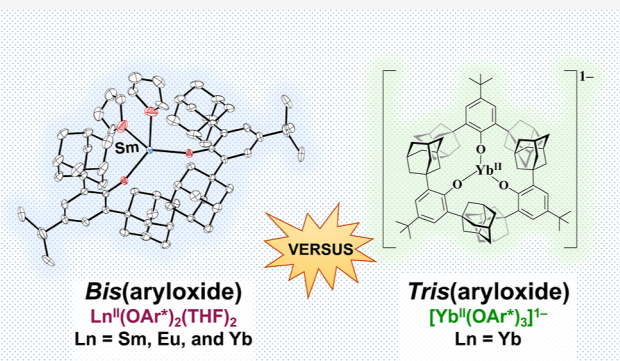
ACCESS |

Metrics & More

Article Recommendations

Supporting Information

ABSTRACT: The syntheses of Ln(II) *bis*(aryloxide) complexes of Sm, Eu, and Yb have been examined with the bulky aryloxide ligand $(OC_6H_2-2,6-Ad_2-4-tBu)^{1-}$ $[(OAr^*)^{1-}$; Ad = 1-adamantyl]. These $Ln^{II}(OAr^*)_2(THF)_2$ complexes were pursued for comparison with the *tris*(aryloxide) Ln(II) complexes $[Ln^{II}(OAr^*)_3]^{1-}$ ($Ln = La, Ce, Nd, Gd, Dy, and Lu$), which have $4f^n5d^1$ electron configurations, and with $4f^{14} [Yb^{II}(OAr^*)_3]^{1-}$. Although the Ln(II) chemistry of Sm, Eu, and Yb is often similar since they all adopt $4f^{n+1}$ electron configurations, their chemistry is surprisingly diverse with $(OAr^*)^{1-}$. Reactions of $Ln^{II}I_2(THF)_2$ with $KOAr^*$ in THF form the *bis*(aryloxide) Ln(II) complexes $Ln^{II}(OAr^*)_2(THF)_2$, **1-Ln**, that were characterized by X-ray diffraction for **1-Sm** and **1-Yb**, but crystals of **1-Eu** have been elusive. Reduction of the *tris*(aryloxide) Sm(III) complex, $Sm^{III}(OAr^*)_3$, **2-Sm**, prepared from $Sm^{III}(NR_2)_3$ ($R = SiMe_3$) and $HOAr^*$ in refluxing toluene, generated the *bis*(aryloxide) complex, **1-Sm**, and $KOAr^*$ rather than a Sm analogue of $[Yb^{II}(OAr^*)_3]^{1-}$. Reduction of $Eu^{III}(OAr^*)_3$, **2-Eu**, prepared from $EuCl_3$ with $KOAr^*$ in THF, caused an immediate dark blue-purple to bright red-orange color change, but crystals of the product were elusive. Neither reduction of $Tm^{III}(OAr^*)_3$, **2-Tm**, nor the reaction of $Tm^{II}I_2(DME)_3$ with $KOAr^*$ provided crystalline Tm(II) complexes.



INTRODUCTION

Recently, a new series of Ln(II) complexes for $Ln = La, Ce, Nd, Gd, Dy, Yb$, and Lu supported by the bulky aryloxide ligand $(OAr^*)^{1-}$ $[(OAr^*)^{1-} = (OC_6H_2-2,6-Ad_2-4-tBu)^{1-}$; Ad = 1-adamantyl] was reported.¹ The $[Ln^{II}(OAr^*)_3]^{1-}$ complexes of La, Ce, Nd, Gd, Dy, and Lu, formed by reduction of the $4f^n Ln^{III}(OAr^*)_3$ complexes, adopt $4f^n5d^1$ electron configurations and exhibit enhanced thermal stability compared to other Ln(II) complexes of the general formula $(Ln^{II}A_3)^{1-}$, where A is an anionic ligand such as cyclopentadienyl or amide, that also adopt these unusual electron configurations.^{1–6} The $4f^{14}$ Yb(II) complex, $[K(crypt)][Yb^{II}(OAr^*)_3]$ (crypt = 2,2,2-cryptand), was also reported and proved to be the most stable Ln(II) complex of the series.¹ In light of these findings, it was of interest to study the $(OAr^*)^{1-}$ ligand with other lanthanide metals known to adopt traditional $4f^{n+1}$ electron configurations for comparison. Specifically, we sought Ln(II) complexes of Sm, Eu, and Tm, since these ions traditionally adopt $4f^6$, $4f^7$, and $4f^{13}$ electron configurations, respectively. The Ln(II) complexes of these metals have the additional feature that they can potentially be accessed from $Ln^{II}I_2$ precursors, which are not available for the other lanthanide metals. Aryloxide complexes of Eu(II),^{7,8} Yb(II),^{8,9} and Sm(II),^{10–13} with ligands such as $(OC_6H_2-tBu_2-2,6-Me-4)^{1-}$ and $(OC_6H_2-tBu_3-2,4,6)^{1-}$ have previously been reported in the literature.¹⁴

Herein, we report a new class of Ln(II) $(OAr^*)^{1-}$ complexes in which only two aryloxide ligands are attached to the metal: $Ln^{II}(OAr^*)_2(THF)_2$, **1-Ln**, for $Ln = Sm, Eu$, and Yb. We also describe the unexpected subtle variations reported between these three metals (as well as with Tm) in this ligand system in terms of synthesis, crystallizability, and $Ln^{II}(OAr^*)_2(THF)_2$ versus $[Ln^{II}(OAr^*)_3]^{1-}$ stability.

RESULTS

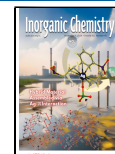
Synthesis of Bis(Aryloxide) Complexes from $Ln^{II}I_2(THF)_x$ ($Ln = Eu, Sm$, and Yb). Salt metathesis reactions between $Ln^{II}I_2(THF)_x$ reagents and $KOAr^*$ were initially examined to determine if the *bis*(aryloxide) complexes $Ln^{II}(OAr^*)_2(THF)_2$ ($OAr^* = OC_6H_2-2,6-Ad_2-4-tBu$; Ad = 1-adamantyl), **1-Ln**, could be synthesized similarly to other Eu(II)⁷ and Yb(II)⁸ aryloxide complexes¹⁴ and the *bis*(cyclopentadienyl) complexes $Cp^*_2Ln^{II}(THF)_2$ ($Cp^* = C_5Me_5$; $x = 0–2$) for $Ln = Sm, Eu$, and Yb, which form from reactions of

Received: August 5, 2024

Revised: October 13, 2024

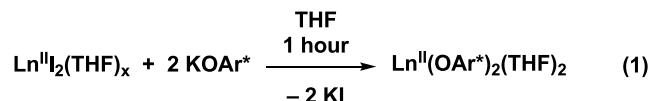
Accepted: October 18, 2024

Published: October 29, 2024



the sterically bulky pentamethylcyclopentadienide reagent KCp^* and $\text{Ln}^{\text{II}}\text{I}_2(\text{THF})_x$.^{15–17} The desired potassium reagent KOAr^* was synthesized in 91% yield upon workup by reacting HOAr^* with $\text{K}[\text{N}(\text{SiMe}_3)_2]$ in toluene at room temperature. The diiodide precursors of Sm, Eu, and Yb, $\text{Ln}^{\text{II}}\text{I}_2(\text{THF})_2$, were synthesized according to literature preparations from Ln^0 metal shavings and 1,2-diiodoethane in THF.^{18,19}

The addition of a THF solution of KOAr^* to a stirred THF solution of $\text{Yb}^{\text{II}}\text{I}_2(\text{THF})_x$ at room temperature generates an opaque maroon solution after 1 h, **eq 1**. Centrifugation



$\text{Ln} = \text{Sm, Eu, Yb; } x = 2–3$
 $\text{KOAr}^* = \text{KOC}_6\text{H}_2\text{Ad}_2\text{-2,6-}^t\text{Bu-4;}$
 $\text{Ad} = 1\text{-adamantyl}$

1-Ln

followed by removal of solvent under reduced pressure yields $\text{Yb}^{\text{II}}(\text{OAr}^*)_2(\text{THF})_2$, **1-Yb**, as a maroon solid in 94% yield. Maroon crystals of **1-Yb** suitable for X-ray diffraction studies were obtained by slow vapor diffusion of hexanes into THF at -18°C and the complex has the structure as shown in **Figure 1**.

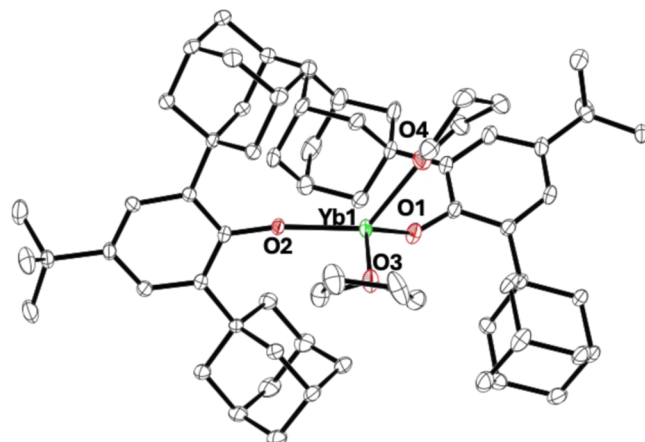


Figure 1. Molecular structure of $\text{Yb}^{\text{II}}(\text{OAr}^*)_2(\text{THF})_2$, **1-Yb**, with selective atom labeling. Ellipsoids are drawn at the 50% probability level and hydrogen atoms are not shown for clarity. The molecular structure of **1-Sm** is similar to that of **1-Yb**, although the two $(\text{OAr}^*)^{1-}$ ligands are crystallographically equivalent in **1-Sm**, as are the two THF molecules.

Similarly, the room temperature reaction of $\text{Sm}^{\text{II}}\text{I}_2(\text{THF})_x$ with KOAr^* in THF generates an opaque purple solution after 1 h and yields $\text{Sm}^{\text{II}}(\text{OAr}^*)_2(\text{THF})_2$, **1-Sm**, as a purple solid in 86% yield upon workup. The structure was again definitively identified by X-ray crystallography. Selected metrical parameters for **1-Sm** and **1-Yb** are reported in **Table 1**.

When $\text{Eu}^{\text{II}}\text{I}_2(\text{THF})_2$ reacts with KOAr^* in a THF/hexane mixture at room temperature, an opaque bright orange solution is generated. Centrifugation followed by removal of solvent under reduced pressure yields an orange oil of what is hypothesized to be $\text{Eu}^{\text{II}}(\text{OAr}^*)_2(\text{THF})_2$, **1-Eu**. However, single crystals suitable for X-ray crystallography have remained elusive despite the fact that the similarly sized samarium analogue crystallizes readily and complexes of two 2,6-di-*tert*-butylaryloxide ligands with Eu(II) have previously been

Table 1. Selected Bond Distances (Å) and Angles (deg) of $\text{Ln}(\text{OAr}^*)_2(\text{THF})_2$, 1-Ln^a

metrics (Å or deg)	1-Sm	1-Yb	$[\text{K}(\text{crypt})][\text{Yb}(\text{OAr}^*)_3]$
$\text{Ln}-\text{O}_{\text{OAr}^*}$	2.268(1)	2.174(2) 2.158(2)	2.182(1)–2.189(1)
$\text{Ln}-\text{O}_{\text{THF}}$	2.526(2)	2.390(3) 2.385(3)	
$\text{O}_{\text{OAr}^*}-\text{Ln}-\text{O}_{\text{THF}}$	93.07(8)	95.37(10) 95.45(9)	
$\text{O}_{\text{OAr}^*}-\text{Ln}-\text{O}_{\text{OAr}^*}$	125.47(9)	120.70(8)	119.96(2)
$\text{Ln}-\text{O}-\text{C}_{\text{ipso}}$	156.42(7)	168.99(1) 133.94(1)	147.56(4)
τ_4	1	0.74	
$G (\%)$	87	88	91

^aThe Guzei G value assess the steric saturation about the metal center and is reported as a percentage, with a G value of 100% correlating to a fully sterically saturated metal center.³⁰

crystallographically characterized, i.e., $\text{Eu}^{\text{II}}(\text{OC}_6\text{H}_3^t\text{Bu}_2\text{-2,6})_2(\text{THF})_3$ ²⁰ and $\text{Eu}^{\text{II}}(\text{OC}_6\text{H}_2\text{-Me-4-}^t\text{Bu}_2\text{-2,6})_2(\text{THF})_3$.²¹

Attempts to synthesize the analogous $\text{Tm}(\text{II})$ *bis*(aryloxide) complex $\text{Tm}^{\text{II}}(\text{OAr}^*)_2$ were made using the DME-solvated precursor $\text{Tm}^{\text{II}}\text{I}_2(\text{DME})_3$ (DME = 1,2-dimethoxyethane) previously reported by Bochkarev and co-workers.²² An immediate color change from dark green to brown is observed when a solution of KOAr^* in rigorously dried DME is added to a stirred solution of $\text{TmI}_2(\text{DME})_2$ at room temperature. However, only colorless crystals of HOAr^* and dark green crystals of $\text{TmI}_2(\text{DME})_3$ were obtained upon workup.

Structure of $\text{Ln}^{\text{II}}(\text{OAr}^*)_2(\text{THF})_2$, 1-Ln. Selected metric data for **1-Sm** and **1-Yb** are reported in **Table 1**. Complex **1-Yb** crystallizes in the $P2_1/c$ space group with one molecule of THF in the asymmetric unit. The four oxygen atoms bound to the Yb metal center adopt a distorted tetrahedral geometry with $\tau_4 = 0.73$. The average $\text{Yb}-\text{O}$ aryloxide distance of 2.164(1) Å is shorter than the average 2.224(7) Å $\text{Yb}-\text{O}$ distances of $\text{Yb}^{\text{II}}(\text{OAr})_2(\text{NCMe})_4$ ²⁰ ($\text{OAr} = \text{OC}_6\text{H}_3^t\text{Bu}_2\text{-2,6}$) which is consistent with the larger coordination number for the latter compound. However, the $\text{Yb}-\text{O}$ distance of **1-Yb** is also shorter than the 2.2232(7) Å $\text{Yb}-\text{O}$ distance in $\text{Yb}^{\text{II}}(\text{OAr}')_2(\text{THF})_2$ ($\text{OAr}' = \text{OC}_6\text{H}_2^t\text{Bu}_2\text{-2,6-Me-4}$),²³ which has the same coordination number and a smaller aryloxide ligand. Another curious aspect of the structure of **1-Yb** is that the two $\text{Yb}-\text{O}-\text{C}_{\text{ipso}}$ angles are very different, 168.99(8)° for O(1) and 133.94(1)° for O(2), even though the 2.174(2) and 2.158(2) Å $\text{Yb}-\text{O}$ distances are similar. The 130.50(9)° and 125.06(9)° $\text{O}_{\text{Ar}^*}-\text{Yb}-\text{O}_{\text{Ar}^*}$ angles of **1-Yb** are much larger than the 108.2(4)° and 118.7(3)° $\text{O}_{\text{Ar}}-\text{Yb}-\text{O}_{\text{Ar}}$ angles of $\text{Yb}^{\text{II}}(\text{OAr})_2(\text{NCMe})_4$ and $\text{Yb}^{\text{II}}(\text{OAr}')_2(\text{THF})_2$, respectively.^{20,23} The metrical parameters in **1-Yb** put the four adamantyl groups in a roughly tetrahedral orientation. The closest H···H distance between two adamantyl groups in **1-Yb**, 2.16 Å, is shorter than twice the 1.2 van der Waals radius of a hydrogen atom, suggesting that dispersion forces between the bulky groups^{24,25} may be present in the structure.

The four oxygen atoms in **1-Sm** adopt a more regular tetrahedral geometry, with $\tau_4 = 1.0$. The **1-Sm** complex crystallizes in the $C2/c$ space group with the asymmetric unit containing just one $(\text{OAr}^*)^{1-}$ ligand and one THF molecule. The $\text{Sm}-\text{O}_{\text{OAr}^*}$ distance of 2.268(2) Å is shorter than the 2.339(8) Å analogue of $\text{Sm}^{\text{II}}(\text{OAr}')_2(\text{THF})_3$ ²⁶ and the 2.302(4) Å distance in $\text{Sm}^{\text{II}}(\text{OAr}^{\text{OMe}})_2(\text{THF})_3$ ($\text{OAr}^{\text{OMe}} =$

$\text{OC}_6\text{H}_2\text{-}2,6\text{-Bu}^t\text{-}4\text{-OMe}$,²⁷ both of which have larger coordination numbers. The 2.309(1) Å Sm–O distance in $\text{Sm}^{\text{II}}(\text{OAr}^{\text{Pr}6})_2$ [$\text{Ar}^{\text{Pr}6} = -\text{C}_6\text{H}_3\text{-}2,6\text{-}(\text{C}_6\text{H}_2\text{-}2,4,6\text{-Pr}_3)_2$],²⁸ which has arene as well as aryloxide coordination, is also larger. The $\text{Ln}^{\text{II}}\text{-O}$ distances of **1-Sm** and **1-Yb** are similar to one another when the 0.14 Å difference in seven-coordinate $\text{Ln}(\text{II})$ ionic radii of the two ions is considered, Table 1.²⁹ The symmetry equivalent Sm–O–C_{ipso} angle in **1-Sm**, 156.42(7)°, is close to the average of the disparate 168.99(8)° and 133.94(1)° values in **1-Yb**. Similar to **1-Yb**, a short H···H distance of 2.38 Å is observed between two adamantly groups of **1-Sm** and suggests the presence of dispersion forces in crystalline **1-Sm**.^{24,25}

The Guzei G parameters, which assess the steric saturation of the metal center and are reported as percentages,³⁰ are 87 and 88% for **1-Sm** and **1-Yb**, respectively. These numbers are in the high range observed for stable rare-earth metal complexes, Table 1. For example, $[\text{Yb}^{\text{II}}(\text{OAr}^*)_3]^{1-}$ has a G value of 91% and 2.182(1)–2.189(1) Å Yb–O distances that are similar to the 2.164(1) Å distance in **1-Yb**.¹

Spectroscopy of $\text{Ln}^{\text{II}}(\text{OAr}^*)_2(\text{THF})_2$, **1-Ln, Complexes.** The UV–vis spectra of **1-Eu** and **1-Yb** in THF each contain a single broad absorbance around 360 nm with extinction coefficients of 1500 and 370 $\text{M}^{-1} \text{cm}^{-1}$, respectively, as shown in Figure 2. The UV–vis spectrum of **1-Sm** in THF shows

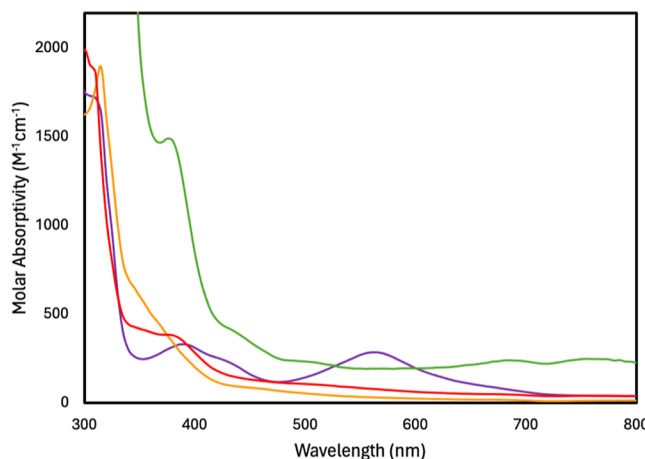


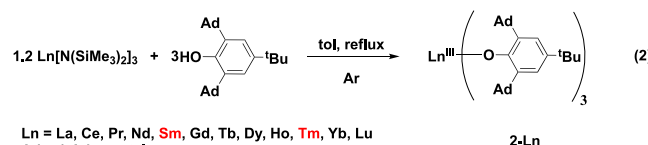
Figure 2. UV–vis spectra of **1-Sm** (purple), **1-Eu** (orange), **1-Yb** (red), and $[\text{Yb}^{\text{II}}(\text{OAr}^*)_3]^{1-}$ (green).

three absorbances at 390, 435, and 560 nm with extinction coefficients of 330, 220, and 290 $\text{M}^{-1} \text{cm}^{-1}$, respectively, as shown in Figure 2. The extinction coefficient magnitudes for **1-Sm**, **1-Eu**, and **1-Yb** are lower than the 1200–9000 $\text{M}^{-1} \text{cm}^{-1}$ values observed for the $4\text{f}^m5\text{d}^1$ $\text{Ln}(\text{II})$ complexes $[\text{Ln}^{\text{II}}(\text{OAr}^*)_3]^{1-}$ and are consistent with other Sm(II), Eu(II), and Yb(II) complexes in the literature. Comparative examples include $\text{Yb}^{\text{II}}\text{I}_2(\text{THF})_{2,5}$,³¹ $\text{Yb}^{\text{II}}[\text{N}(\text{SiPr}_3)_2]_2$,³² $\text{Sm}^{\text{II}}[\text{N}(\text{SiPr}_3)_2]_2$,³² and $\text{Sm}^{\text{II}}(\text{crown})\text{I}_2$ ³¹ (crown = 18-crown-6). The UV–vis spectra of the 4f^{n+1} $\text{Ln}(\text{II})$ complexes **1-Sm**, **1-Eu**, and **1-Yb** are plotted alongside the 4f^{14} Yb(II) complex $[\text{K}(\text{crypt})][\text{Yb}^{\text{II}}(\text{OAr}^*)_3]$ in Figure 2 for comparison.

Synthesis and Reduction of $\text{Ln}^{\text{III}}(\text{OAr}^*)_3$ Complexes, **2-Ln.** It was of interest to examine the reduction of the tris(aryloxide) complexes $\text{Ln}^{\text{III}}(\text{OAr}^*)_3$, **2-Ln**, of Sm, Eu, and Tm to determine whether they would form $\text{Ln}(\text{II})$ tris(aryloxide) complexes, namely $[\text{Ln}^{\text{II}}(\text{OAr}^*)_3]^{1-}$, or the $\text{Ln}(\text{II})$ bis(aryloxide) complexes, **1-Ln**. Previously, we reported

that the reduction of $\text{Yb}^{\text{III}}(\text{OAr}^*)_3$ with KC_8 and in the presence of crypt yields the most thermally stable $\text{Ln}(\text{II})$ tris(aryloxide) complex of the series, $[\text{K}(\text{crypt})][\text{Yb}^{\text{II}}(\text{OAr}^*)_3]$.¹

The synthetic route employed for the synthesis of $\text{Sm}^{\text{III}}(\text{OAr}^*)_3$, **2-Sm**, and $\text{Tm}^{\text{II}}(\text{OAr}^*)_3$, **2-Tm**, was the same as that used to generate the $\text{Ln}^{\text{III}}(\text{OAr}^*)_3$, **2-Ln**, complexes of $\text{Ln} = \text{Y}$, La, Ce, Nd, Gd, Dy, Ho, Tm, Yb, and Lu, namely the protonolysis of $\text{Ln}^{\text{III}}(\text{NR}_2)_3$ ($\text{R} = \text{SiMe}_3$) with three equivalents of HOAr^* in toluene at reflux, eq 2.¹



Bright yellow crystals of **2-Sm** and colorless crystals of **2-Tm** suitable for X-ray diffraction studies were grown overnight from concentrated hexane solutions stored in a –35 °C freezer. Both complexes crystallize in the $P2_1/n$ space group, but **2-Sm** has one hexane molecule and one molecule of pentane in the asymmetric unit, while **2-Eu** has two molecules of hexane. The crystal structure of **2-Sm** is shown in Figure 3.

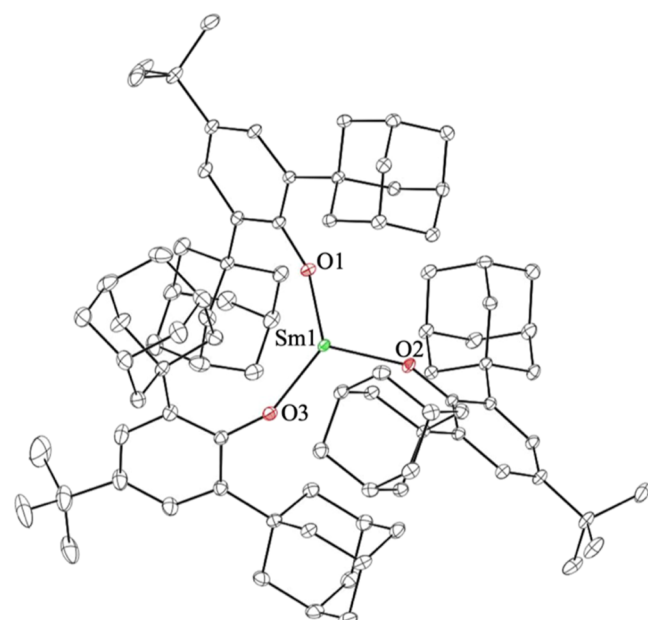


Figure 3. Molecular structure of $\text{Sm}^{\text{III}}(\text{OAr}^*)_3$, **2-Sm**, with selective atom labeling. Ellipsoids are drawn at the 50% probability level. Hydrogen atoms and solvent molecules are not shown for clarity.

Since the synthesis of pure samples of the starting material $\text{Eu}^{\text{III}}(\text{NR}_2)_3$ is problematic due to formation of the Eu(II) complexes $[\text{Li}^+][\text{Eu}^{\text{II}}(\text{NR}_2)_3]$ and $\text{Eu}^{\text{II}}(\text{NR}_2)_2(\text{THF})_2$,^{33,34} $\text{Eu}^{\text{III}}(\text{OAr}^*)_3$, **2-Eu**, was synthesized from EuCl_3 and three equivalents of KOAr^* in THF at room temperature. This reaction yields a dark blue solution after stirring at room temperature for 1 h. Upon workup, **2-Eu** was isolated as a dark blue solid in 88% yield. Dark blue crystals of **2-Eu** were obtained overnight from a concentrated pentane solution. Like **2-Sm** and **2-Tm**, **2-Eu** crystallizes in the $P2_1/n$ space group and has pseudo- C_3 symmetry about the Ln metal center, but it has two molecules of pentane in the asymmetric unit. Selected bond metrics for **2-Ln** are reported in Table 2. Although there

Table 2. Selected Bond Distances (Å) and Angles (deg) of $\text{Ln}(\text{OAr}^*)_3$, 2-Ln^a

metrics (Å or deg)	2-Sm	2-Eu	2-Tm
average $\text{Ln}-\text{O}$	2.099(2)–2.120(2)	2.083(2)–2.105(2)	2.011(2)–2.030(2)
$\text{O}-\text{Ln}-\text{O}$	113.12(8)–121.34(8)	113.360(9)–121.430(7)	108.56(8)–122.05(8)
average $\text{Ln}-\text{O}-\text{C}_{\text{ipso}}$	148.27(1)	149.15(1)	148.26(3)
δ ($\text{Ln}-\text{O}_3$ plane)	0.393	0.385	0.443
G (%)	90	91	92

^a δ is the displacement (Å) of the metal center from the O_3 plane of the three aryloxide ligands.

is no evidence of residual HOAr^* present in the crystals, the IR spectra of **2-Tm** and **2-Eu** show the presence of a weak signal around 3600 cm^{-1} that is attributed to a small amount of unreacted HOAr^* . A similar signal was observed for **1-Yb** and other previously reported $\text{Ln}(\text{III})$ complexes supported by $(\text{OAr}^*)^{1-}$.¹

The **2-Sm**, **2-Eu**, and **2-Tm** complexes are structurally similar but not isomorphous since they each crystallize in different unit cells and contain a different number of solvent molecules in the asymmetric unit. The structural similarities of the three **2-Ln** compounds are exemplified by the $\text{O}-\text{Ln}-\text{O}$ and $\text{Ln}-\text{O}-\text{C}_{\text{ipso}}$ angles, which vary little between the three complexes, 108.56(8)–122.05(8) and 148.26(3)–149.15(1), respectively. The $\text{Ln}-\text{O}$ distances of **2-Sm**, **2-Eu**, and **2-Tm** are also in agreement with the $\text{Ln}-\text{O}$ distances previously reported for $\text{Ln} = \text{Y}$, La , Ce , Nd , Dy , Gd , and Lu when the differences in metal ionic radii are taken into account.²⁹ All three complexes show a slight pyramidalization of the metal center with respect to the three bound oxygen atoms, similar to what was previously observed for the other $\text{Ln}^{(\text{III})}(\text{OAr}^*)_3$ complexes.

Reduction of 2-Sm, 2-Eu, and 2-Tm. Previous studies showed that reduction of $\text{Yb}^{(\text{III})}(\text{OAr}^*)_3$, **2-Yb**, with KC_8 in THF and in the presence of crypt at -35°C forms the *tris*(aryloxide) complex $[\text{K}(\text{crypt})][\text{Yb}^{(\text{II})}(\text{OAr}^*)_3]$, **2-Yb**, and not the *bis*(aryloxide) complex $\text{Yb}^{(\text{II})}(\text{OAr}^*)_2(\text{THF})_2$, **1-Yb**.¹ Multiple attempts were made to synthesize an analogous $[\text{Sm}^{(\text{II})}(\text{OAr}^*)_3]^{1-}$ complex from *tris*(aryloxide) complex **2-Sm**. Reductions of bright orange **2-Sm** in THF or Et_2O at -35°C and in the presence of either crypt or crown produced purple solutions that quickly faded to gold, as an insoluble purple solid was formed that could not be characterized further spectroscopically. However, the reduction of **2-Sm** with a potassium smear in cold THF formed a dark purple solution with absorbances at 390, 435, and 560 nm that resemble those of **1-Sm**, Figure S25. Storage of the dark purple solution in a -35°C freezer for 1 week yields dark purple triangular crystals, which were different in morphology from **1-Sm**. However, attempts to perform X-ray diffraction studies on several occasions proved to be unsuccessful. Similar results were obtained when the analogous reduction was performed in Et_2O .

When **2-Eu** is treated with KC_8 in cold Et_2O and in the presence of crypt, an immediate color change from dark blue to orange was observed. Upon filtration, an orange solution with a UV-vis spectrum similar to that of **1-Eu**, shown in Figure S26, was obtained. However, like the product of the reaction of $\text{Eu}^{(\text{II})}\text{I}_2(\text{THF})_2$ with KOAr , no crystalline material was isolated. Interestingly, no color change was observed when reduction of **2-Eu** was attempted in cold THF.

The reaction of **2-Tm** and KC_8 in either cold Et_2O or cold THF and in the presence of either crypt or crown yields a dark gray solution after 10 min in a -35°C freezer. The UV-vis

spectrum of this solution shows three absorbances at 410, 465, and 565 nm with molar absorptivities of 710, 430, and 540 $\text{M}^{-1} \text{ cm}^{-1}$, respectively, as shown in Figure S27. Although this spectrum has similarities with that of the $\text{Tm}(\text{II})$ complex $\text{Tm}^{(\text{II})}[\text{N}(\text{Si}^i\text{Pr}_3)_2]_2$, which exhibits three absorbances in the UV-vis region with molar absorptivities between 800 and 1500 $\text{M}^{-1} \text{ cm}^{-1}$,³¹ no crystals were obtained to confirm the identity of the reduction product.

■ DISCUSSION

The *bis*(aryloxide) $\text{Ln}(\text{II})$ complexes $\text{Ln}^{(\text{II})}(\text{OAr}^*)_2(\text{THF})_2$, **1-Ln**, can be readily synthesized and crystallographically analyzed for $\text{Ln} = \text{Sm}$ and Yb . An analogous product with spectroscopic features consistent with **1-Eu** can also be obtained, but it did not form crystals suitable for X-ray crystallography, despite the similar sizes of Sm and Eu . These two elements usually have similar chemistry and the $\text{Eu}(\text{II})$ complexes are typically less difficult to isolate than those of the more reducing $\text{Sm}(\text{II})$ complex. The chemistry of $\text{Tm}(\text{II})$ also differed from that of similarly sized $\text{Yb}(\text{II})$, although $\text{Tm}(\text{II})$ is much more reactive and does not always behave like $\text{Yb}(\text{II})$.

Although both $\text{Yb}^{(\text{II})}(\text{OAr}^*)_2(\text{THF})_2$, **1-Yb**, and $[\text{K}(\text{crypt})][\text{Yb}^{(\text{II})}(\text{OAr}^*)_3]$ are known, attempts to synthesize crystallizable $[\text{Ln}^{(\text{II})}(\text{OAr}^*)_3]^{1-}$ complexes for Sm , Eu , and Tm were unsuccessful. For Sm and Eu , reductions of $\text{Ln}^{(\text{III})}(\text{OAr}^*)_3$, **2-Ln**, form solutions with UV-vis spectra consistent with the presence of $\text{Ln}^{(\text{II})}(\text{OAr}^*)_2(\text{THF})_2$, **1-Ln**, but no crystallizable products. It should be noted, that although the $\text{Ln}(\text{II})$ *bis*(cyclopentadienyl) complexes $\text{Cp}^*_2\text{Ln}^{(\text{II})}(\text{THF})_2$ ($\text{Cp}^* = \text{C}_5\text{Me}_5$) of Sm , Eu , and Yb are readily accessible,^{15–17} the *tris*(cyclopentadienyl) $\text{Ln}(\text{II})$ complexes ($\text{Cp}^*_3\text{Ln}^{(\text{II})})^{1-}$ of these metals have remained elusive. The potassium reduction of $\text{Cp}^*_3\text{Sm}^{(\text{III})}$ forms $\text{Cp}^*_2\text{Sm}^{(\text{II})}$ and KCP^* .³⁵ The reduction of $\text{Ln}^{(\text{III})}(\text{OAr}^*)_3$, **2-Ln**, for Sm and Eu appears to parallel that reactivity.

■ CONCLUSIONS

Exploration of the traditional $\text{Ln}(\text{II})$ ions of Sm , Eu , Tm , and Yb , which typically have $4f^{n+1}$ electron configurations, for comparison with $[\text{K}(\text{crypt})][\text{Ln}^{(\text{II})}(\text{OAr}^*)_3]$ complexes of the other lanthanides that have $4f^n5d^1$ configurations, provided unexpectedly diverse results. Frequently, the similarly sized lanthanide metal ions $\text{Sm}(\text{II})$ and $\text{Eu}(\text{II})$ as well as $\text{Tm}(\text{II})$ and $\text{Yb}(\text{II})$ form analogous complexes with X-ray crystal structures that differ only in the small difference in size of the metal ions. Differences do occur in the reduction chemistry within each pair since the reduction potentials of $\text{Sm}(\text{II})$ and $\text{Tm}(\text{II})$ are much more negative than those of $\text{Eu}(\text{II})$ and $\text{Yb}(\text{II})$, respectively. However, with the $(\text{OAr}^*)^{1-}$ ligand, structural isomorphs between the metal pairs were not isolated. These results add to the intricacies of the $(\text{OAr}^*)^{1-}$ ligand and its coordination chemistry with the lanthanides. For the $\text{Ln}^{(\text{III})}(\text{OAr}^*)_3$ and $[\text{K}(\text{crypt})][\text{Ln}^{(\text{II})}(\text{OAr}^*)_3]$ complexes, similar

structural and chemical behavior is observed within each series, except for $[K(\text{crypt})][\text{Ce}^{\text{II}}(\text{OAr}^*)_3]$ which is much less stable than its analogues. Hence, it appears that for both traditional $4f^{n+1}$ and nontraditional $4f^n5d^1$ $\text{Ln}(\text{II})$ complexes of the $(\text{OAr}^*)^{1-}$ ligand, the chemistry is not completely governed by steric saturation effects that should lead to similar chemistry for complexes of metals with similar size.

EXPERIMENTAL SECTION

All manipulations and syntheses described below were conducted with the rigorous exclusion of air and water using standard Schlenk line and glovebox techniques under an argon atmosphere. Solvents were sparged with UHP argon and dried by passage through columns containing Q-5 and molecular sieves prior to use.³⁶ Deuterated NMR solvents were degassed and dried over molecular sieves for 1 week. All ^1H and $^{13}\text{C}\{^1\text{H}\}$ NMR spectra were recorded on ADVANCE600 MHz spectrometers at 298 K and referenced internally to residual protio-solvent resonances. It should be noted that a spectral window of +160 to -160 ppm was used for the collection of all ^1H NMR spectra and a spectral window of +300 to -200 ppm was used for the collection of all ^{13}C NMR spectra. UV-vis spectra were collected in Et_2O at room temperature in a 0.1 cm Schlenk cuvette fitted with a Teflon stopcock by using an Agilent Cary 60 UV-vis spectrometer unless stated otherwise. IR transmittance measurements were taken as compressed solids on an Agilent Cary 630 FTIR spectrophotometer with a diamond ATR attachment. Elemental analyses were conducted on a Thermo Scientific FlashSmart CHNS/O elemental analyzer at UC Irvine Materials Research Institute's TEMPR facility in Irvine, California. 2,2,2-Cryptand (crypt) and 18-crown-6 (crown) were purchased from Sigma-Aldrich and recrystallized in Et_2O prior to use. HOAr^* ,³⁷ $\text{Ln}^{\text{II}}\text{I}_2(\text{THF})_2(\text{THF})_x$,^{15–17} $\text{Ln}^{\text{III}}(\text{NR}_2)_3$ ($\text{R} = \text{SiMe}_3$)³⁸, and KC_8 ³⁹ were synthesized using published preparations. *Caution!* KC_8 is a known pyrophoric reagent and appropriate precautions were taken when handling this material.

KOAr^{*}. In an argon-containing glovebox, HOAr^* (2.00 g, 4.78 mmol) and $\text{K}[\text{N}(\text{SiMe}_3)_2]$ (0.953 g, 4.78 mmol) were combined in 100 mL of toluene and left to stir at room temperature. Over the course of 1 day, the initial clear yellow solution had turned opaque white. The resulting solution was filtered through a medium porosity glass frit to yield white solids that were first washed with toluene (10 mL) and then with hexanes (30 mL). The solids were collected and dried under reduced pressure to yield KOAr^* as white powdery solids (1.99 g, 91%). ^1H NMR ($\text{THF}-d_8$, 600 MHz): δ , ppm 6.71 (s, 2H, *m*-H), 2.31 (s, 12H, Ad-CH₂), 1.98 (s, 6H, Ad-CH), 1.79 (m, 12H, Ad-CH₂), 1.21 (s, 9H, ¹Bu). ^{13}C NMR (C_6D_6 , 151 MHz): δ , ppm = 159.20 (*i*-C), 138.31 (*o*-C), 129.50 (*p*-C), 119.81 (*m*-C), 41.54 (Ad-CH₂), 38.92 (quaternary C from either ¹Bu or Ad), 38.17 (Ad-CH₂), 34.50 (quaternary C from ¹Bu or Ad), 32.83 (CMe₃), 30.86 (Ad-CH). IR (cm⁻¹): 2900s, 2842s, 2670w, 2649w, 1762w, 1589w, 1436s, 1386w sh, 1359m, 1337m, 1307s, 1271m, 1241s, 1198w, 1173m, 1099m, 1053m, 976m, 899w sh, 878m, 822m, 817m, 800w, 782w, 721m, 691w, 659w.

Sm^{II}(OAr^{*})₂(THF)₂, 1-Sm. A THF solution of KOAr^* (251 mg, 0.549 mmol) was added dropwise to a stirred THF solution of $\text{SmI}_2(\text{THF})_2$ (150 mg, 0.275 mmol). An immediate color change from clear dark blue to opaque purple-brown was observed upon addition of KOAr^* . After stirring at room temperature for 1 h, the solution was centrifuged to yield a dark purple supernatant and white solids. The purple supernatant was dried under *vacuo* to yield $\text{Sm}^{\text{II}}(\text{OAr}^*)_2(\text{THF})_2$, 1-Sm, as flakey purple/black solids (267 mg, 86%). Single crystals of 1-Sm suitable for X-ray diffraction studies were grown by the slow vapor diffusion of hexanes into a concentrated THF solution of 1-Sm at -35 °C over 1 month. ^1H NMR ($\text{THF}-d_8$, 600 MHz): δ , ppm 7.37, 5.06, 3.25, 2.22, 2.02, 1.72, 1.41, 1.12, 0.88, 0.29. ^{13}C NMR (C_6D_6 , 151 MHz): δ , ppm 152.46, 141.69, 135.31, 121.45, 41.31, 36.95, 34.54, 31.75, 29.24. IR (cm⁻¹): 2894s, 2842s, 2675w, 2654w, 1595w, 1422s, 1386w sh, 1359m, 1342m, 1309w sh, 1277s, 1236s, 1197w sh, 1173w, 1132w, 1096m, 1051s, 973m, 894m, 872m, 833s, 820m, 804m, 779m, 757w, 726m, 656w. UV-vis (THF,

room temperature) λ_{max} nm (ϵ , M⁻¹ cm⁻¹): 390 (330), 435 (220), 560 (290). Anal. Calcd for $\text{Sm}(\text{OAr}^*)_2(\text{THF})_2$: C, 72.41; H, 8.58. Found: C, 72.63; H, 8.21.

Eu^{II}(OAr^{*})₂, 1-Eu. $\text{Eu}^{\text{II}}\text{I}_2(\text{THF})_2$ (150 mg, 0.274 mmol) was reacted with KOAr^* (250 mg, 0.547 mmol) as described above for 1-Sm. An immediate color change from clear purple to opaque orange was observed upon the addition of KOAr^* . After stirring at room temperature for one h, the solution was centrifuged to yield an orange supernatant and white solids. Drying the supernatant under *vacuo* yields 1-Eu as an oily dark orange solid (270 mg, 89%). ^1H NMR ($\text{THF}-d_8$, 600 MHz): δ , ppm 7.36 (s, 2H, *m*-CH), 7.16 (s, residual HOAr^{*}), 5.04 (s, residual HOAr^{*}), 2.21 (m, 12H, Ad-CH₂), 1.69 (s, 6H, Ad-CH), 1.38 (m, 12H, Ad-CH₂), 0.88 (s, 9H, ¹Bu). ^{13}C NMR (C_6D_6 , 151 MHz): δ , ppm = 41.34, 36.98, 31.83, 29.21. IR (cm⁻¹): 2951m sh, 2894s, 2842s, 2677w, 2653w, 1594w, 1529m, 1469w sh, 1447m, 1425m, 1389w sh, 1356m, 1340m, 1313w, 1279m, 1236m, 1197w, 1165w, 1129w, 1096w, 1096m sh, 1055s, 1031s, 976m, 940w, 891m, 872m, 831m, 815m, 803m, 776w, 754w, 726m, 691w, 656w. UV-vis (THF, room temperature) λ_{max} nm (ϵ , M⁻¹ cm⁻¹): 350 (1500). Anal. Calcd for $\text{Eu}(\text{OAr}^*)_2(\text{THF})_2$: C, 72.31; H, 8.57. Found: C, 72.78; H, 8.93.

Yb^{II}(OAr^{*})₂(THF)₂, 1-Yb. A THF solution of KOAr^* (241 mg, 0.527 mmol) was added dropwise to a stirred THF solution of $\text{Yb}^{\text{II}}\text{I}_2(\text{THF})_2$ (150 mg, 0.264 mmol). An immediate color change from clear yellow to opaque maroon was observed upon the addition of KOAr^* . After stirring at room temperature for one h, the solution was centrifuged to yield a vibrant maroon supernatant and white solids. The maroon supernatant was dried under *vacuo* to yield $\text{Yb}^{\text{II}}(\text{OAr}^*)_2(\text{THF})_2$, 1-Yb, as flakey red-brown solids (286 mg, 94%). Single crystals of 1-Yb suitable for X-ray diffraction studies were grown by slow vapor diffusion of hexanes into a concentrated THF solution of 1-Yb at -35 °C over 2 weeks. ^1H NMR ($\text{THF}-d_8$, 600 MHz): δ , ppm 6.93 (s, 2H, *m*-H), 6.81 (s, residual HOAr^{*}), 5.68 (s, residual HOAr^{*}), 3.61 (m, 2H, THF), 2.26 (m, 6H, Ad-CH₂), 2.19 (m, 6H, Ad-CH₂), 2.04 (m, 6H, Ad-CH), 1.82 (m, 2H, THF), 1.78 (m, 12H, Ad-CH₂), 1.26 (s, 9H, ¹Bu), 1.21 (m, residual HOAr^{*}). ^{13}C NMR ($\text{THF}-d_8$, 151 MHz): δ , ppm 120.40, 119.62, 67.25, 42.12, 42.04, 41.00, 37.71, 37.59, 37.48, 37.11, 31.76, 31.58, 31.25, 29.66, 29.56, 25.40. IR (cm⁻¹): 2896s, 2879s, 2676w, 2654w, 1595w, 1428s, 1401w sh, 1411m, 1357m, 1344m sh, 1278s, 1239s, 1221w, 1200w, 1155w, 1100m, 1096w sh, 1053m, 1025m, 1012m, 874m, 837m, 829m, 813m, 790w, 723m, 714m, 662m. UV-vis (THF, room temperature) λ_{max} nm (ϵ , M⁻¹ cm⁻¹): 387 (370). Anal. Calcd for $\text{Yb}(\text{OAr}^*)_2(\text{THF})_2$: C, 70.99; H, 8.41. Found: C, 73.06; H, 8.88. Multiple attempts were made to get better analytical data without success.⁴⁰

Sm^{III}(OAr^{*})₃, 2-Sm. $\text{Sm}^{\text{III}}[\text{N}(\text{SiMe}_3)_2]_3$ (200 mg, 0.317 mmol) and HOAr^* (331 mg, 0.792 mmol) were combined in toluene (40 mL) in a 100 mL Schlenk flask containing a Teflon-coated stir bar and fitted with a Teflon stopcock. The sealed clear yellow solution was stirred at reflux for 2 days to yield a cloudy bright yellow-orange solution. Solvent was removed under reduced pressure to yield bright orange oily solids. These solids were dissolved in 20 mL of hexanes, transferred to a 25 mL scintillation vial, and then redried under reduced pressure to yield oily, bright yellow solids. Washing the oily solids with pentane (3 × 4 mL) and then drying under *vacuo* yields $\text{Sm}^{\text{III}}(\text{OAr}^*)_3$, 2-Sm, as a chalky yellow solid (230 mg, 62%). Single crystals of 2-Sm suitable for X-ray diffraction studies could be grown overnight from a concentrated hexane solution in a -35 °C freezer. ^1H NMR (C_6D_6 , 600 MHz): δ , ppm 8.71, 2.74, 2.21, 2.13, 2.11, 2.02, 1.98, 1.73, 1.41, 1.25, 1.11, 0.88, 0.37, 0.10, -0.03. ^{13}C NMR (C_6D_6 , 151 MHz): δ , ppm 153.52, 143.06, 141.17, 138.88, 136.92, 130.34, 129.60, 129.53, 126.75, 126.70, 122.89, 66.98, 46.22, 42.69, 42.28, 39.11, 38.40, 37.36, 37.03, 33.62, 33.15, 31.28, 30.63, 29.14, 26.74, 24.13, 22.44, 21.97, 16.69, 15.45, 3.71. IR (cm⁻¹): 2900s, 2848s, 2675w, 2651w, 1745w, 1597w, 1444m sh, 1427s, 1391w, 1359m, 1343m, 1340m, 1314w, 1279m, 1241m sh, 1225s, 1201m, 1140m, 1102m, 1045w, 1011w, 978m, 924m, 872m, 837s, 809s, 769s, 731s, 693w, 662w. UV-vis (THF, room temperature) λ_{max} nm (ϵ , M⁻¹ cm⁻¹): 389 (840). Anal. Calcd for $\text{Sm}(\text{OAr}^*)_3$: C, 77.03; H, 8.83.

Found: C, 75.02; H, 9.14. Multiple attempts were made to get better analytical data without success.⁴⁰

Eu^{III}(OAr^{*})₃, 2-Eu. Eu^{III}Cl₃ (200 mg, 0.774 mmol) was reacted with KOAr^{*} (1.06 g, 2.32 mmol) in THF at room temperature to yield a dark red solution. Centrifugation followed by removal of solvent under a vacuum yields a chalky red-purple solid that was then triturated with *n*-hexanes (15 mL) and redried under vacuo to yield 2-Eu as a purple solid in 88% yield. Crystals of 2-Eu suitable for X-ray crystallography were grown overnight by dissolving these solids in minimal hexanes and storing in a 35 °C freezer. ¹H NMR (C₆D₆, 600 MHz): δ, ppm 16.50, 10.77, 7.37, 5.06, 3.28, 2.21, 2.03, 1.59, 1.42, 1.23, 0.88, -1.94, -3.89. ¹³C NMR (C₆D₆, 151 MHz): δ, ppm 141.90, 135.65, 121.79, 116.09, 67.95, 64.11, 41.59, 37.32, 36.33, 35.03, 32.06, 29.52, 27.97, 25.74, 23.08, 22.71, 20.79, 18.87, 17.70, 14.29, 11.51. IR (cm⁻¹): 3632w, 2899s, 2839s, 2672w, 2645w, 1753w, 1594w, 1443s, 1422s, 1389w, 1359m, 1339m, 1323w sh, 1312m, 1276s, 1252w sh, 1238m sh, 1225s, 1197m, 1181w, 1167m, 1129w, 1099m, 1074m, 1044w, 976m, 937w, 918w, 896w, 866m, 833s, 814m, 800m, 762m, 757w sh, 727m, 707w, 655w. UV-vis (THF, room temperature) λ_{max} nm (ϵ , M⁻¹ cm⁻¹): 495 (300). UV-vis (*n*-hexanes, room temperature) λ_{max} nm (ϵ , M⁻¹ cm⁻¹): 580 (300). Anal. Calcd for Eu(OAr^{*})₃: C, 79.04; H, 9.12. Found: C, 79.34; H, 9.67.

Tm^{III}(OAr^{*})₃, 2-Tm. Tm^{III}[N(SiMe₃)₂]₃ (200 mg, 0.316 mmol) was reacted with HOAr^{*} (331 mg, 0.790 mmol) as described above for 2-Sm for 2 days to yield a cloudy yellow solution. The solvent was removed under reduced pressure to yield oily yellow solids. Crystals of 2-Tm suitable for X-ray crystallography were grown overnight by dissolving these solids in minimal hexanes and storing in a -35 °C freezer. ¹H NMR (C₆D₆, 600 MHz): δ, ppm 7.38, 5.06, 3.28, 2.23, 2.11, 2.04, 1.80, 1.73, 1.59, 1.49, 1.43, 1.25, 1.14, 1.03, 0.98, 0.91, 0.12. ¹³C NMR (C₆D₆, 151 MHz): δ, ppm 136.36, 121.41, 41.15, 37.07, 34.55, 31.54, 29.21, 25.40, 25.19, 22.42, 14.95, 13.88. IR (cm⁻¹): 3386w, 2898s, 2846s, 1598w, 1445m sh, 1426s, 1387w, 1354m, 1338m, 1308w, 1275m, 1258m, 1242s, 1228s, 1200m, 1181w, 1134w, 1098w, 1076w, 1043w, 975m, 925m, 873m, 843w, 818w, 810w, 771w, 763m, 735m, 710w, 691w, 655w. Anal. Calcd for Tm(OAr^{*})₃: C, 76.02; H, 8.72. Found: C, 76.26; H, 9.39.

X-ray Crystallographic Data. CCDC entries 2359872, 2359871, 2363974, 2365680, and 2365681 contain the supplementary crystallographic data for this paper. These data can be obtained free of charge via www.ccdc.cam.ac.uk/data_request/cif, or by emailing data_request@ccdc.cam.ac.uk, or by contacting The Cambridge Crystallographic Data Centre, 12 Union Road, Cambridge CB2 1EZ, UK; Fax: +44-1223-336033. Crystal data, bond length and angle tables, and structure refinement information can be found in the Supporting Information.

ASSOCIATED CONTENT

Supporting Information

The Supporting Information is available free of charge at <https://pubs.acs.org/doi/10.1021/acs.inorgchem.4c03332>.

Additional experimental details on the reductions of the *tris*-aryloxide complexes 2-Ln, ¹H and ¹³C NMR spectra, IR spectra, UV-vis spectra, and crystallographic details for all compounds (PDF) ([PDF](#))

Accession Codes

Deposition numbers 2359871–2359872, 2363974, and 2365680–2365681 contain the supplementary crystallographic data for this paper. These data can be obtained free of charge via the joint Cambridge Crystallographic Data Centre (CCDC) and Fachinformationszentrum Karlsruhe Access Structures service.

AUTHOR INFORMATION

Corresponding Author

William J. Evans – Department of Chemistry, University of California, Irvine, California 92697-2025, United States; orcid.org/0000-0002-0651-418X; Email: wevans@uci.edu

Authors

Lauren M. Anderson-Sanchez – Department of Chemistry, University of California, Irvine, California 92697-2025, United States; orcid.org/0000-0002-9697-8008

Joseph W. Ziller – Department of Chemistry, University of California, Irvine, California 92697-2025, United States; orcid.org/0000-0001-7404-950X

Complete contact information is available at: <https://pubs.acs.org/10.1021/acs.inorgchem.4c03332>

Notes

The authors declare no competing financial interest.

ACKNOWLEDGMENTS

We thank the U.S. National Science Foundation for support of this research under CHE-2154255.

REFERENCES

- Anderson-Sanchez, L. M.; Yu, J. M.; Ziller, J. W.; Furche, F.; Evans, W. J. Room-Temperature Stable Ln(II) Complexes Supported by 2,6-Diadamantyl Aryloxide Ligands. *Inorg. Chem.* **2023**, *62*, 706–714.
- Moehring, S. A.; Beltrán-Leiva, M. J.; Páez-Hernández, D.; Arratia-Pérez, R.; Ziller, J. W.; Evans, W. J. Rare-Earth Metal(II) Aryloxides: Structure, Synthesis, and EPR Spectroscopy of [K(2,2,2-cryptand)][Sc(OC₆H₄Bu₂-2,6-Me-4)₃]. *Chem.—Eur. J.* **2018**, *24*, 18059–18067.
- Moehring, S. A.; Miehlich, M.; Hoerger, C. J.; Meyer, K.; Ziller, J. W.; Evans, W. J. A Room-Temperature Stable Y(II) Aryloxide: Using Steric Saturation to Kinetically Stabilize Y(II) Complexes. *Inorg. Chem.* **2020**, *59* (5), 3207–3214.
- Fieser, M. E.; MacDonald, M. R.; Krull, B. T.; Bates, J. E.; Ziller, J. W.; Furche, F.; Evans, W. J. Structural, Spectroscopic, and Theoretical Comparison of Traditional vs Recently Discovered Ln²⁺ Ions in the [K(2,2,2-cryptand)][(C₅H₄SiMe₃)₃Ln] Complexes: The Variable Nature of Dy²⁺ and Nd²⁺. *J. Am. Chem. Soc.* **2015**, *137*, 369–382.
- Ryan, A. J.; Darago, L. E.; Balasubramani, S. G.; Chen, G. P.; Ziller, J. W.; Furche, F.; Long, J. R.; Evans, W. J. Synthesis, Structure, and Magnetism of Tris(amide) {Ln[N(SiMe₃)₂]₃}¹⁻ Complexes of the Non-Traditional + 2 Lanthanide Ions. *Chem.—Eur. J.* **2018**, *24*, 7702–7709.
- Ryan, A. J.; Ziller, J. W.; Evans, W. J. The Importance of the Counter-cation in Reductive Rare-Earth Metal Chemistry: 18-Crown-6 Instead of 2,2,2-Cryptand Allows Isolation of [Y^{II}(NR₂)₃]¹⁻ and Ynediolate and Enediolate Complexes from CO Reactions. *Chem. Sci.* **2020**, *11*, 2006–2014.
- van den Hende, J. R.; Hitchcock, P. B.; Holmes, S. A.; Lappert, M. F.; Leung, W.-P.; Mak, T. C.; Prashar, S. Synthesis and characterisation of lanthanide(II) aryloxides including the first structurally characterised europium(II) compound [Eu(OC₆H₄Bu₂-2,6-Me-4)₂(thf)₃]·thf (thf = tetrahydrofuran). *J. Chem. Soc., Dalton Trans.* **1995**, 1427–1433.
- Carretas, J.; Branco, J.; Marçalo, J.; Domingos, A. ~; Pires de Matos, A. Europium(II) and ytterbium(II) aryloxide chemistry: synthesis and crystal structure of [Eu(OC₆H₃Bu₂-2,6)₂(THF)₃·0.75C₇H₈] and [Yb(OC₆H₃Bu₂-2,6)₂(NCMe)₄]. *Polyhedron* **2003**, *22*, 1425–1429.

(9) van den Hende, J. R.; Hitchcock, P. B.; Holmes, S. A.; Lappert, M. F. Synthesis and ^{171}Yb - $\{^1\text{H}\}$ nuclear magnetic resonance spectra of ytterbium(II) aryloxides $[\text{Yb}(\text{OR}')_2(\text{L})_n]$ [$(\text{L})_n = (\text{OEt}_2)_2$, (thf)₂, (thf)₃, (pyridine)₂ or $\text{Me}_2\text{PCH}_2\text{CH}_2\text{PMe}_2$] and $[\{\text{Yb}(\mu\text{-OR}')(\text{X})_2\}(\text{X} = \text{OR}' \text{ or } \text{NR}_2)(\text{R}' = \text{C}_6\text{H}_2\text{Bu}'_2\text{-2,6-Me-4}, \text{R} = \text{SiMe}_3)$; thf = tetrahydrofuran]. *J. Chem. Soc., Dalton Trans.* **1995**, 1435–1440.

(10) Qj, G.-Z.; Shen, Q.; Lin, Y.-H. A bis(2,6-di-tert-butyl-4-methylphenolato)samarium(II) complex, $[\text{Sm}(\text{OAr})_2(\text{thf})_3]\text{thf}$. *Acta Crystallogr., Sect. C: Cryst. Struct. Commun.* **1994**, C50, 1456–1458.

(11) Hou, Z.; Fujita, A.; Yoshimura, T.; Jesorka, A.; Zhang, Y.; Yamazaki, H.; Wakatsuki, Y. Heteroleptic Lanthanide Complexes with Aryloxide Ligands. Synthesis and Structural Characterization of Divalent and Trivalent Samarium Aryloxide/Halide and Aryloxide/Cyclopentadienide Complexes. *Inorg. Chem.* **1996**, 35, 7190–7195.

(12) Zhao, P.; Zhu, Q.; Fettinger, J. C.; Power, P. Characterization of a Monomeric, Homoleptic, Solvent-Free Samarium Bis(aryloxide). *Inorg. Chem.* **2018**, 57, 14044–14046.

(13) Deacon, G. B.; Fallon, G. D.; Forsyth, C. M.; Harris, S. C.; Junk, P. C.; Skelton, B. W.; White, A. H. Manipulation of reaction pathways in redox transmetallation-ligand exchange syntheses of lanthanoid(II)/(III) aryloxide complexes. *Dalton Trans.* **2006**, 802–812.

(14) Boyle, T. J.; Ottley, L. A. M. Advances in Structurally Characterized Lanthanide Alkoxide, Aryloxide, and Silyloxide Compounds. *Chem. Rev.* **2008**, 108, 1896–1917.

(15) Evans, W. J.; Grate, J. W.; Choi, H. W.; Bloom, I.; Hunter, W. E.; Atwood, J. L. Solution synthesis and crystallographic characterization of the divalent organosamarium complexes $(\text{C}_5\text{Me}_5)_2\text{Sm}(\text{THF})_2$ and $[(\text{C}_5\text{Me}_5)_2\text{Sm}(\mu\text{-I})(\text{THF})_2]_2$. *J. Am. Chem. Soc.* **1985**, 107, 941–946.

(16) Evans, W. J.; Hughes, L. A.; Hanusa, T. P. Synthesis and x-ray crystal structure of bis(pentamethylcyclopentadienyl) complexes of samarium and europium: $(\text{C}_5\text{Me}_5)_2\text{Sm}$ and $(\text{C}_5\text{Me}_5)_2\text{Eu}$. *Organometallics* **1986**, 5, 1285–1291.

(17) Tilley, T. D.; Andersen, R. A.; Spencer, B.; Ruben, H.; Zalkin, A.; Templeton, D. H. Divalent Lanthanide Chemistry. Bis(pentamethylcyclopentadienyl)europium(II) and -ytterbium(II) Derivatives: Crystal Structure of Bis(pentamethylcyclopentadienyl)-(tetrahydrofuran)ytterbium(II)-Hemitoluene at 176 K. *Inorg. Chem.* **1980**, 19, 2999–3003.

(18) Girard, P.; Namy, J. L.; Kagan, H. B. Divalent lanthanide derivatives in organic synthesis. 1. Mild preparation of samarium iodide and ytterbium iodide and their use as reducing or coupling agents. *J. Am. Chem. Soc.* **1980**, 102, 2693–2698.

(19) Heckmann, G.; Niemeyer, M. Synthesis and First Structural Characterization of Lanthanide(II) Aryls: Observation of a Schlenk Equilibrium in Europium(II) and Ytterbium(II) Chemistry. *J. Am. Chem. Soc.* **2000**, 122, 4227–4228.

(20) Carretas, J.; Branco, J.; Marçalo, J.; Domingos, A.; Pires de Matos, A. Europium(II) and ytterbium(II) aryloxide chemistry: synthesis and crystal structure of $[\text{Eu}(\text{OC}_6\text{H}_3\text{Bu}'_2\text{-2,6})_2(\text{THF})_3\bullet 0.75\text{C}_7\text{H}_8]$ and $[\text{Yb}(\text{OC}_6\text{H}_3\text{Bu}'_2\text{-2,6})_2(\text{NCMe})_4]$. *Polyhedron* **2003**, 22, 1425–1429.

(21) Deacon, G. B.; Hamidi, S.; Junk, P. C.; Kelly, R. P.; Wang, J. Direct Reactions of Iodine-Activated Rare-Earth Metals with Phenols of Varying Steric Bulk. *Eur. J. Inorg. Chem.* **2014**, 2014, 460–468.

(22) Bochkarev, M. N.; Fedushkin, I. L.; Fagin, A. A.; Petrovskaya, T. V.; Ziller, J. W.; Broomhall-Dillard, R. N. R.; Evans, W. J. The First Discreet Thulium(II) Complex: $[\text{TmI}_2(\text{MeOCH}_2\text{CH}_2\text{OMe})_3]$. *Angew. Chem.* **1997**, 109, 123–125.

(23) Van den Hende, J. R.; Hitchcock, P. B.; Lappert, M. F. Three-coordinate Neutral Ligand-free Ytterbium(II) Complexes $[\{\text{YbX}(\mu\text{-X})_2\}]$ ($\text{X} = \text{OAr}$ **1** or OCBu'_3 **3**) or $[\{\text{Yb}(\text{NR}_2)(\mu\text{-X})_2\}]$ ($\text{X} = \text{OCBu}'_3$ **2** or OAr **4**) ($\text{Ar} = \text{C}_6\text{H}_2\text{Bu}'_2\text{-2,6-Me-4}$, $\text{R} = \text{SiMe}_3$); the X-Ray Structures of **1** and **2**. *J. Chem. Soc., Chem. Commun.* **1994**, 1413–1414.

(24) Liptrot, D. J.; Power, P. P. London dispersion forces in sterically crowded inorganic and organometallic molecules. *Nat. Rev. Chem.* **2017**, 1, 0004.

(25) Linus, P. *The Nature of the Chemical Bond*; Cornell University Press: Ithaca, 1960.

(26) Hou, Z.; Fujita, A.; Yoshimura, T.; Jesorka, A.; Zhang, Y.; Yamazaki, H.; Wakatsuki, Y. Heteroleptic Lanthanide Complexes with Aryloxide Ligands. Synthesis and Structural Characterization of Divalent and Trivalent Samarium Aryloxide/Halide and Aryloxide/Cyclopentadienide Complexes. *Inorg. Chem.* **1996**, 35, 7190–7195.

(27) Deacon, G. B.; Fallon, G. D.; Forsyth, C. M.; Harris, S. C.; Junk, P. C.; Skelton, B. W.; White, A. H. Manipulation of reaction pathways in redox transmetallation-ligand exchange syntheses of lanthanoid(II)/(III) aryloxide complexes. *Dalton Trans.* **2006**, 802–812.

(28) Zhao, P.; Zhu, Q.; Fettinger, J. C.; Power, P. Characterization of a Monomeric, Homoleptic, Solvent-Free Samarium Bis(aryloxide). *Inorg. Chem.* **2018**, 57, 14044–14046.

(29) Shannon, R. D. Revised effective ionic radii and systematic studies of interatomic distances in halides and chalcogenides. *Acta Crystallogr. Sect. A Cryst. Phys. Diff. Theor. Gen. Crystallogr.* **1976**, 32, 751–767.

(30) Guzei, I. A.; Wendt, M. An Improved Method for the Computation of Ligand Steric Effects Based on Solid Angles. *Dalton Trans.* **2006**, 3991–3999.

(31) Goodwin, C. A. P.; Chilton, N. F.; Vettese, G. F.; Moreno Pineda, E.; Crowe, I. F.; Ziller, J. W.; Winpenny, R. E. P.; Evans, W. J.; Mills, D. P. Physicochemical Properties of Near-Linear Lanthanide(II) Bis(silylamine) Complexes ($\text{Ln} = \text{Sm, Eu, Tm, Yb}$). *Inorg. Chem.* **2016**, 55, 10057–10067.

(32) Namy, J.-L.; Colomb, M.; Kagan, H. B. Samarium Diiodide in Tetrahydropyran: Preparation and some Reactions in Organic Chemistry. *Tetrahedron Lett.* **1994**, 35, 1723–1726.

(33) Li, H.-X.; Xu, Q. F.; Chen, J. X.; Cheng, M. L.; Zhang, Y.; Zhang, W. H.; Lang, J. P.; Shen, Q. Syntheses, crystal structures and catalytic properties of a series of lanthanide(III) bis(trimethylsilyl)-amide chloro complexes: $[(\{\text{Me}_3\text{Si}\}_2\text{N})_2\text{Nd}(\mu\text{-Cl})\text{Li}(\text{THF})_3](\mu\text{-Cl})_2$, $[(\{\text{Me}_3\text{Si}\}_2\text{N})_2\text{Ln}(\mu\text{-Cl})\text{Li}(\text{THF})_2](\mu_3\text{-Cl})_2$ ($\text{Ln} = \text{Eu, Ho}$), and $[(\{\text{Me}_3\text{Si}\}_2\text{N})_2\text{Ln}(\mu\text{-Cl})_2\text{Li}(\text{THF})_2](\mu\text{-Cl})_2$ ($\text{Ln} = \text{Nd, Sm, Eu, Ho, Yb}$). *J. Organomet. Chem.* **2004**, 689, 3438–3448.

(34) Evans, W. J.; Drummond, D. K.; Zhang, H.; Atwood, J. L. Synthesis and x-ray crystal structure of the divalent [bis(trimethylsilyl)amido] samarium complexes $[(\text{Me}_3\text{Si})_2\text{N}]_2\text{Sm}(\text{THF})_2$ and $[(\text{Me}_3\text{Si})_2\text{N}]\text{Sm}(\mu\text{-I})(\text{DME})(\text{THF})_2$. *Inorg. Chem.* **1988**, 27, 575–579.

(35) Evans, W. J.; Perotti, J. M.; Kozimor, S. A.; Champagne, T. M.; Davis, B. L.; Nyce, G. W.; Fujimoto, C. H.; Clark, R. D.; Johnston, M. A.; Ziller, J. W. Synthesis and Comparative η^1 -Alkyl and Sterically Induced Reduction Reactivity of $(\text{C}_5\text{Me}_5)_3\text{Ln}$ Complexes of La, Ce, Pr, Nd, and Sm. *Organometallics* **2005**, 24, 3916–3931.

(36) Pangborn, A. B.; Giardello, M. A.; Grubbs, R. H.; Rosen, R. K.; Timmers, F. J. Safe and Convenient Procedure for Solvent Purification. *Organometallics* **1996**, 15, 1518–1520.

(37) Watanabe, T.; Ishida, Y.; Matsuo, T.; Kawaguchi, H. Syntheses and structures of zirconium(iv) complexes supported by 2,6-diadamantylaryloxide ligands and formation of arene-bridged dizirconium complexes with an inverse sandwich structure. *Dalton Trans.* **2010**, 39, 484–491.

(38) Bradley, D. C.; Ghotra, J. S.; Hart, F. A. Three-co-ordination in Lanthanide Chemistry: Tris[bis(trimethylsilyl)amido]lanthanide(III) Compounds. *Chem. Soc., Chem. Commun.* **1972**, 349–350.

(39) Bergbreiter, D. E.; Killough, J. M. Reactions of Potassium-Graphite. *J. Am. Soc.* **1978**, 100 (7), 2126–2134.

(40) Gabbaï, F. P.; Chirik, P. J.; Fogg, D. E.; Meyer, K.; Mindiola, D. J.; Schäfer, L. L.; You, S. L. An Editorial about Elemental Analysis. *Organometallics* **2016**, 35 (19), 3255–3256.